Thermochimica Acta, 83 (1985) 299–307
Elsevier Science Publishers B.V., Amsterdam – Printed in The Netherlands

THERMAL ANALYTICAL TECHNIQUES APPLIED TO THE ANALYSIS OF PROSTATIC CALCULI

ROBERTA CURINI and GIUSEPPE D'ASCENZO
Department of Chemical Sciences, University of Camerino, Camerino (MC) (Italy)

ENRICO CARDARELLI, ANDREA MAGRÍ and ALDO MARINO
Department of Chemistry, University of Rome, Piazzale Aldo Moro, 5, Rome (Italy)

(Received 30 July 1984)

ABSTRACT

Thermogravimetric and differential scanning calorimetric methods by stereoscopic and polarising microscopy to identify the nucleus, and IR spectroscopy and X-ray analysis as ancillary analytical tools are applied to the analysis of prostatic calculi.

INTRODUCTION

The term prostatic calculosis defines a form of lithiasis that originates at the level of the glandular portion of the prostate and is characterized by the presence of concretions inside the acini and the ducts. These concretions form primitively inside the gland, growing in a centrifugal way, and locating at the periphery of the gland, between the cranial and caudal prostate. They are commonly found in both the prostatic lobes.

These concretions are defined endoprostatic calculi in contrast to esoprostatic calculi which originate at the level of the prostatic urethra or derive from the superior urinary tracts [1–3].

The incidence of prostatic calculosis is very high: statistical surveys show the presence of this phenomenon in more than 20% of the adult male population; Fox [4–6] says that it is possible to find the presence of concretions in every adult prostate.

The etiology of prostatic calculosis is not completely clear. According to the more common hypothesis, starchy bodies, that form inside the prostatic acini by degeneration of the epithelial cells, could be the nucleation centers. The nucleus consists, in more than 90% of the calculi analyzed, of calcium phosphate when the outer shell is formed by calcium oxalate mono- or di-hydrate, calcium, magnesium and ammonium phosphates, apatites, uric acid and urates, calcium citrate, cholesterol and mixtures of these com-

0040-6031/85/$03.30

pounds, and can include organic substances such as proteins.

The calculi then grow through prostatic infections or gland hypertrophy, especially since the latter pathology causes obstructions of the channels and then stagnation of the fluids, consequently increasing the concentration of the chemical species by water resorption.

Nucleation and growth are two completely separate conceptions, especially from an aetiopathological point of view. While the study of nucleation, the primary event, is the major point of interest from the clinical point of view to establish the determining cause of calculosis, a study of the structure growth produces data concerning the prostatic fluid modifications that gave rise to the calculus growth.

When a nucleus with a chemical composition different from the outer shell is present in a calculus, it is possible to suppose that the calculus is an expression of two successive pathological phenomena.

Commonly, as in the case of urinary calculi, the existence of a nucleus is neglected and the analytical datum is referred to in terms of percentage of the different chemical compounds present in toto in the calculus, independent of their locations. The sample pretreatment generally adopted almost precludes the possibility of discovering the nucleus; the calculus, in fact, is crushed, the powder thus obtained is mixed and an average sample is analysed.

Prostatic calculi, like urinary calculi, have been studied by many different workers and by many different techniques [1–9], and a critical discussion was made in a previous paper [10].

In order to obtain a highly reliable method for the analysis of prostatic calculi we applied thermogravimetric and differential scanning calorimetric methods, supported by stereoscopic and polarising microscopy to identify the nucleus, and IR spectroscopy and X-ray analysis as ancillary analytical tools.

The study, as previously [10], was carried out in three steps: (a) characterisation of the pure substances by thermal analysis (TG), differential thermogravimetry (DTG), differential thermal analysis (DTA) and differential scanning calorimetry (DSC). This last technique was specifically applied to cholesterol; (b) analysis of synthetic mixtures (as pellets) with a simulated composition of the calculi; (c) analysis of natural prostatic calculi.

The analysis of the natural calculi was carried out after dissection and examination by stereoscopic and polarized microscopy to identify a possible nucleus, which, when present, was isolated and analyzed separately.

EXPERIMENTAL

TG, DTG and DTA curves were obtained using a 990 DuPont instrument with a DTA furnace, useful to 1200°C, and 951 DuPont thermobalance. The

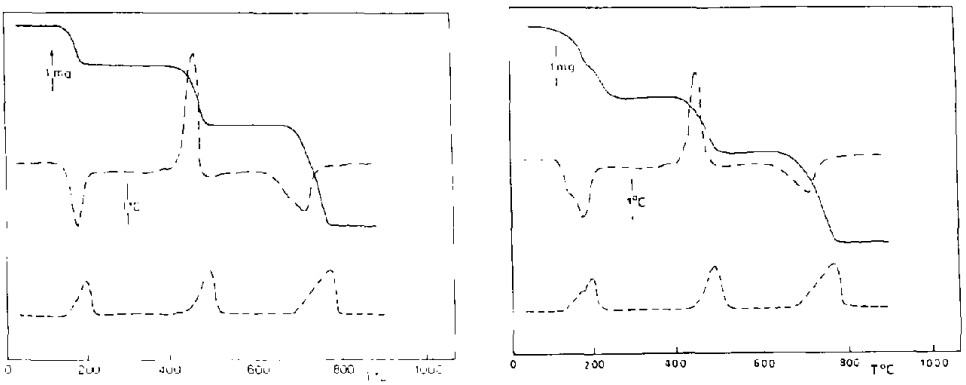

Fig. 1. Calcium oxalate monohydrate. Curves: (———) TG; (- - - - - -) DTG; (·—·—·) DTA. Heating rate, 10°C min^{-1}; atmosphere, air.

Fig. 2. Calcium oxalate dihydrate. Curves and conditions as Fig. 1.

temperature increase ranged between 10 and 50°C min^{-1}. The sample ranged between 1 and 10 mg. The furnace atmosphere was air dried by bubbling in concentrated sulfuric acid, and the gas flow was 50–100 ml min^{-1}.

The DSC curves were obtained using a 990 DuPont instrument equipped with a DSC cell or a DSC-2 Perkin-Elmer instrument equipped with a data station for the analysis of the curves. The temperature increase was 2.5°C min^{-1}. The furnace atmosphere was nitrogen (99.999%), to avoid oxidation phenomena, at the flow rate of 100–200 ml min^{-1}. Cholesterol was supplied from Eastman Organic Chemicals, while all the other reagents were supplied by Merck.

First, the TG, DTG and DTA of the pure substances present in the

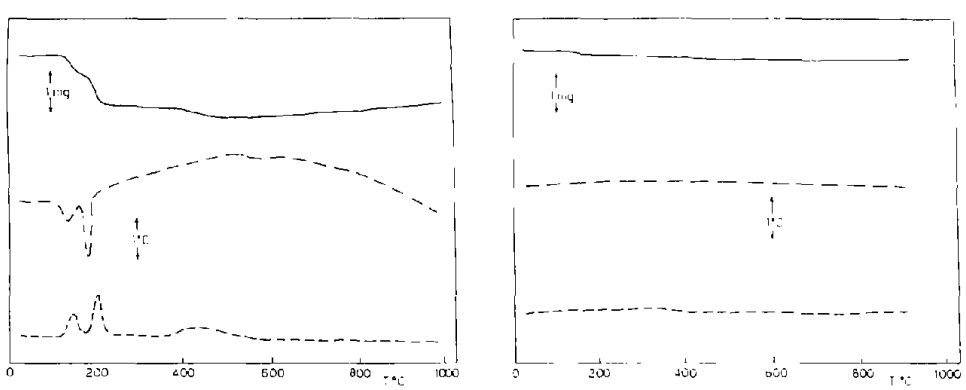

Fig. 3. Calcium hydrogenphosphate dihydrate. Curves and conditions as Fig. 1.

Fig. 4. Apatite. Curves and conditions as Fig. 1.

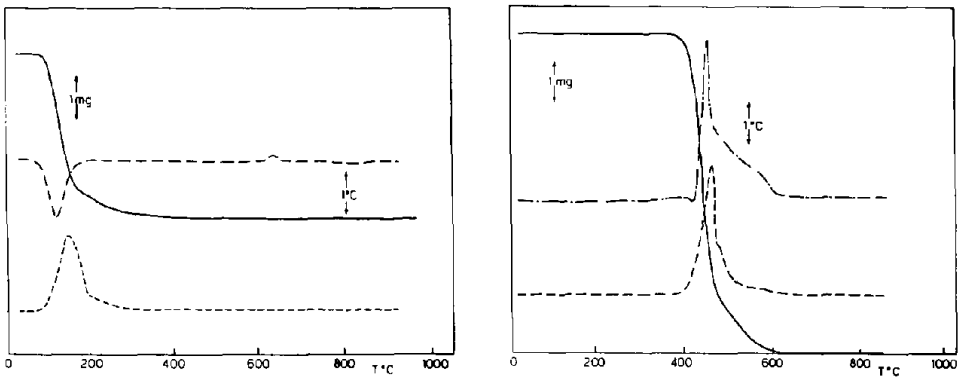

Fig. 5. Ammonium magnesium phosphate hexahydrate. Curves and conditions as Fig. 1.

Fig. 6. Uric acid. Curves and conditions as Fig. 1.

prostatic calculi were carried out. In Figs. 1–7 reproduce the curves of the pure substances that are also present in renal calculi [10], while Figs. 8 and 9 reproduce the curves of the pure substances peculiar to the prostatic calculi. The curves of the pure substances are, if obtained under the same conditions, the standard curves against which the examined samples can be compared.

By weighing the pure substances, after suitable homogenization, pellets were prepared simulating the composition of the natural calculi that were analysed by TG, DTG and DTA. Qualitative analysis was carried out by comparing the curves of the synthetic mixtures with those of the pure substances. Quantitative analysis was carried out as described for the renal calculi [10]. Figures 10 and 11 show an example of the thermoanalytical curves of some synthetic mixtures.

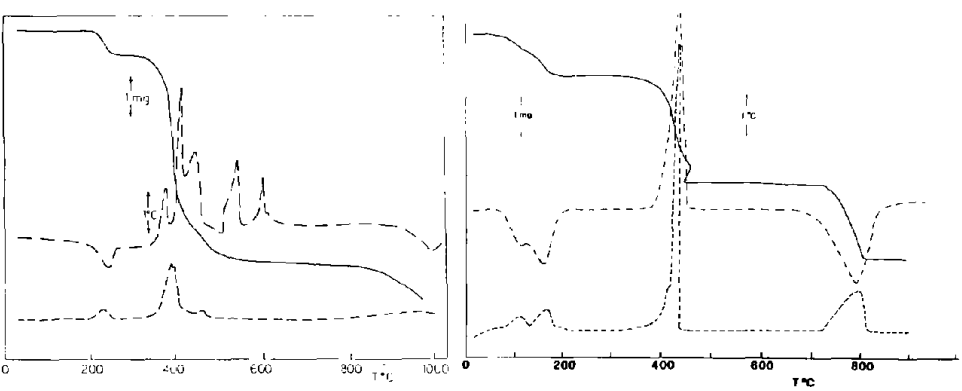

Fig. 7. Monosodium salt of uric acid (monohydrate). Curves and conditions as Fig. 1.

Fig. 8. Calcium citrate dihydrate. Curves and conditions as Fig. 1.

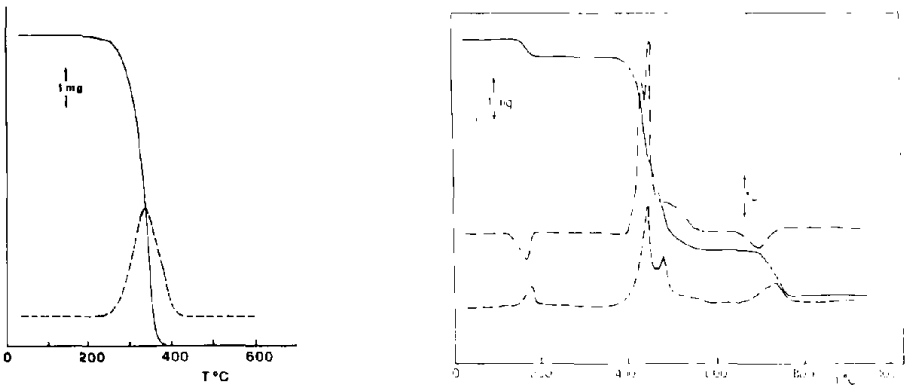

Fig. 9. Cholesterol. Curves: (———) TG; (- - - - - -) DTG. Heating rate, 10°C min^{-1}; atmosphere, air.

Fig. 10. Synthetic mixture of calcium oxalate monohydrate (49.3%) and uric acid (50.7%). Curves and conditions as Fig. 1.

Finally, natural calculi, obtained by surgery, were analyzed. Figure 12 shows an example of the analysis of a calculus. Because the decomposition temperature of cholesterol lies in the temperature range corresponding to the decomposition of the other organic substances present in the calculi, the analysis of the cholesterol was carried out by DSC using the transition phase at 37.5°C [11,12] which is reversible and reproducible (Fig. 13).

To see if a linear correlation between peak area and weight occurred, samples of cholesterol ranging between 0.8 and 12.5 mg were analyzed. To check the reproducibility under the experimental conditions, we submitted

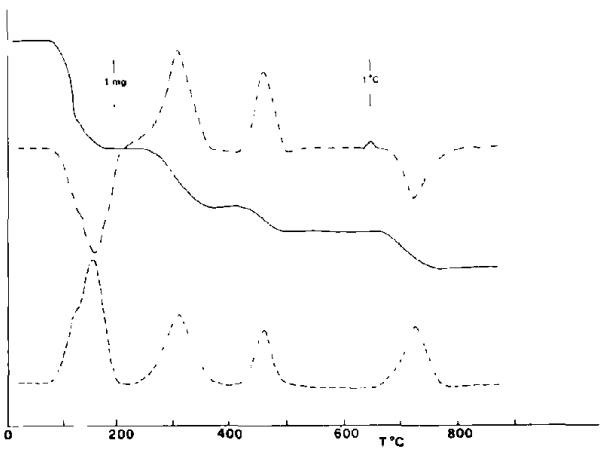

Fig. 11. Synthetic mixture of calcium oxalate monohydrate (32.1%), cholesterol (14.9%) and ammonium magnesium phosphate hexahydrate (53.0%). Curves and conditions as Fig. 1.

each sample to ten heating–cooling cycles and five samples were prepared for each weight.

As shown from Table 1, the values of the linear calibration curve, peak area and amount of sample correlate well: $r = 0.998$. The equation of the regression straight line $y = ax + b$ (y = peak area and x = mg of sample), the standard error on a and b, the standard deviation, SD, the correlation coefficient, r, and the Snedocor parameter, F, were calculated: $a = 0.213 \pm 2.97 \times 10^{-3}$; $b = -3.61 \times 10^{-3} \pm 2.27 \times 10^{-1}$; $SD = 4.13 \times 10^{-2}$; $r = 0.998$; $F = 5.13 \times 10^{-2}$.

The behaviour of the other constituents of the prostatic calculi were then assessed in the DSC and in the temperature field corresponding to the cholesterol transition phase no interfering peaks were observed. Next, syn-

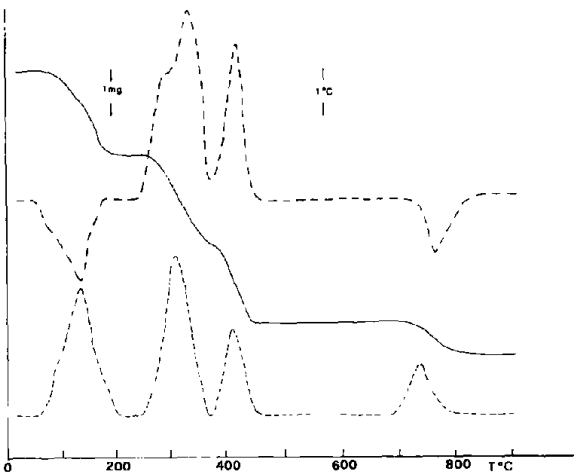

Fig. 12. Calculus of composition: calcium citrate dihydrate (41.2%), cholesterol (12.8%), organic substances (9.7%) and ammonium magnesium phosphate hexahydrate (36.3%). Curves and conditions as Fig. 1.

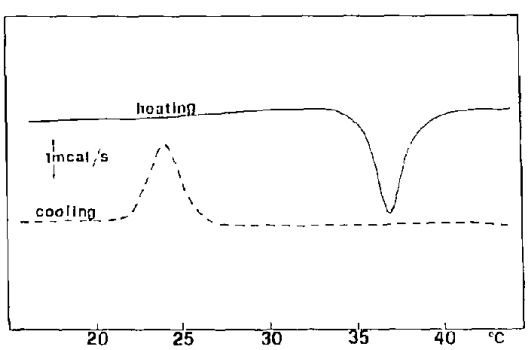

Fig. 13. Cholesterol transition by DSC. Heating rate, 2.5°C min^{-1}; atmosphere, nitrogen.

TABLE 1

Calibration curve data

Cholesterol (mg)	Peak area [a]	SD	CV(%)
0.8	0.13	0.01	7.7
1.7	0.30	0.01	3.3
2.8	0.62	0.02	1.6
3.5	0.77	0.01	1.3
4.6	0.99	0.01	1.0
5.3	1.10	0.02	1.2
5.7	1.25	0.01	0.8
6.2	1.34	0.02	1.5
6.7	1.42	0.01	0.7
6.8	1.44	0.02	1.4
7.4	1.55	0.01	0.6
8.0	1.71	0.02	1.2
8.1	1.76	0.02	1.1
8.6	1.85	0.02	1.0
8.9	1.91	0.02	1.0
9.8	2.04	0.03	1.5
9.9	2.16	0.03	1.4
10.8	2.31	0.02	0.9
11.5	2.33	0.03	1.3
12.1	2.58	0.03	1.2
12.5	2.67	0.03	1.1

[a] Arithmetic means of the areas, obtained as means of ten cycles on each sample, of five samples for each weight.

thetic mixtures with a composition similar to that of the calculi were prepared, to check for any interactions that could give interference. No interferences were found but there was a good agreement between cholesterol present and found. Finally, some calculi from different patients were submitted to parallel analysis by DSC and enzymatic analysis [13] (Table 2).

TABLE 2

Parallel analyses for cholesterol in prostatic calculi by enzymatic analysis [13] and calorimetry

Sample wt. (mg)	Cholesterol found (mg)		Cholesterol found (%)	
	Enz. anal.	Cal. anal.	Enz. anal.	Cal. anal.
97.2	8.7	8.8	8.9	9.0
81.7	12.7	12.8	15.5	15.7
78.5	7.7	7.6	9.8	9.7
84.2	16.5	16.6	19.6	19.7
91.2	8.5	8.5	9.3	9.3
90.5	7.7	7.6	8.5	8.4
88.5	28.0	28.2	31.6	31.9
72.5	6.6	6.6	9.1	9.1

DISCUSSION

The use of thermoanalytical techniques not only allows qualitative and quantitative analyses of the components of the prostatic calculi to be made, but is also useful in determining the crystalline structure of the chemical species and their hydration state. The proposed method, a flow scheme of which is plotted in Fig. 14, requires, as the only pretreatment, the dissection of the calculus and the identification of the nucleus. The analytical time is very short and becomes shorter with the use of a greater temperature increase. Under these conditions, the DTG curve gives a better separation and evidence of the processes, while the TG curve remains perfectly defined and useful for quantitative purposes. Only in the case of very complex calculi is support from ancillary techniques required.

Finally, the method is very reliable, shows an accuracy of about 2% and using appropriate programs the instrumental signals can be directly processed by a computer, thus immediately obtaining the analytical data. The method is useful for routine purposes. More than 100 calculi were analyzed by this method.

ACKNOWLEDGEMENT

This work was supported by the Ministry of Public Instruction of Italy.

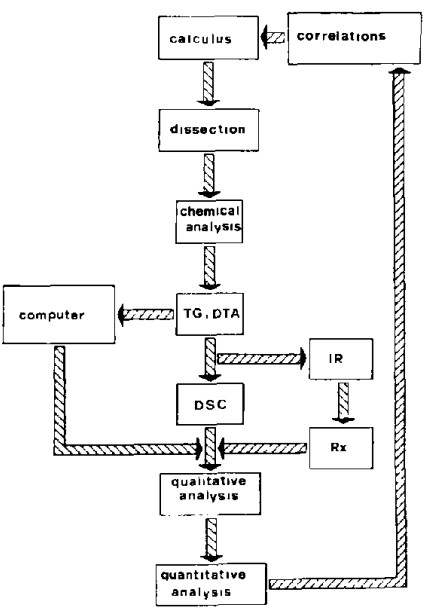

Fig. 14. Flow diagram of the analytical method.

REFERENCES

1 D.J. Sutor and E.S. Wolley, Br. J. Urol., 46 (1974) 533
2 C. Torres Ramirez, J. Aguilar Ruiz, A. Zuluaga Gomez, S. Del Rio Samper and N. Issa Khozouz, Arch. Esp. Urol., 32(6) (1979) 23.
3 C. Torres Ramirez, J. Aguilar Ruiz, A. Zuluaga Gomez, S. Del Rio Samper and J. Passas Martinez, Arch. Esp. Urol., 32(5) (1979) 52.
4 M. Fox, Br. J. Urol., 32 (1960) 458.
5 M. Fox, Br. J. Urol., 34 (1960) 93.
6 M. Fox, J. Urol., 89 (1963) 716.
7 A.J. Leader and D.M. Queen, J. Urol., 80 (1958) 142.
8 C.E. Magura, M. Spector, R. Allen and W.R. Turer, J. Urol., 123 (1980) 294.
9 B. Klein, M. Weissman and J. Berkowitz, Clin. Chem., 6 (1960) 453.
10 G. D'Ascenzo, R. Curini, G. De Angelis, E. Cardarelli, A.D. Magri and L. Miano, Thermochim. Acta, 62 (1983) 149.
11 L.C. Labowitz, Thermochim. Acta, 3 (1972) 419.
12 J.L. Sheumaker and J.K. Guillory, Thermochim. Acta, 5 (1973) 355.
13 I. Roeschlau, E. Bernt and W. Grubea, J. Clin. Chem Clin. Biochem., 12 (1974) 470